THE JOURNAL OF PHYSICAL CHEMISTRY B

ARTICLE

pubs.acs.org/JPCB

Assessment of Dispersion Corrected Atom Centered Pseudopotentials: Application to Energetic Molecular Crystals

Radhakrishnan Balu, Edward F. C. Byrd,* and Betsy M. Rice

U.S. Army Research Laboratory, RDRL-WML-B, Aberdeen Proving Ground, Maryland 21005-5066, United States

Supporting Information

ABSTRACT: A comparative study of the structural features of molecular crystals 1,3,5,7-tetranitro-1,3,5,7-tetraazacyclooctane (HMX), cyclotrimethylenetrinitramine (RDX), 2,4,6-trinitro-1,3,5-benzenetriamine (TATB), and pentaerythritol tetranitrate (PETN) at ambient pressure were calculated using density functional theory (DFT) and dispersion corrected atom centered pseudopotentials (DCACPs). While the molecular structural parameters showed little dependence on the pseudopotential used, the overall volume and lattice vector lengths were substantially improved by the use of DCACPs. DCACP predictions of lattice vector lengths are within 1.3% of experiment, corresponding to an approximately 2% error in density. Conversely, DFT underestimates crystal densities by 5−10%. The results indicate that DCACPs substantially compensate for the inadequate description of van der Waals interactions in DFT. Additionally, comparison of DCACP predictions with analogous calculations using an alternate dispersion corrected DFT method indicate while both show an improvement over traditional DFT methods in describing van der Waals interactions for the molecular crystals in this study, the DCACP method is more accurate in predicting lattice vectors.

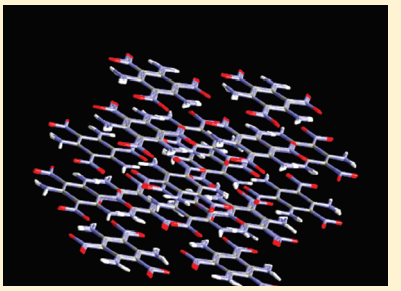

1. INTRODUCTION

The computational design and assessment of new energetic materials can offset some of the higher costs associated with the synthesis, testing, and fielding of these materials. Such computations, however, have practical merit only if their predictive capability leads to an accurate assessment of potential hazards or properties related to performance. The accurate prediction of one of these properties, crystal density, is particularly important since it is used to estimate the performance of a material in gun or warhead applications. Thus, we have expended considerable effort in assessing various theoretical methodologies (classical dynamics and semiempirical and quantum mechanics) to predict this property.[1] Among these methodologies, ab initio methods are the most transferable across systems and have the minimum degree of empiricism, making them the most attractive for use.[2−5]

Ab initio methods based on density functional theory (DFT) are extensively used to treat moderately sized systems (i.e., hundreds to thousands of atoms) due to the computational efficiency they offer. Additionally, DFT predictions show reasonable accuracy for gas-phase molecular systems, and certain condensed-phase materials.[4,5] However, DFT fails to describe adequately systems whose overall interactions have a significant van der Waals (vdW) contribution. Such systems include conventional energetic materials.[6,7] This deficiency in conventional DFT can be traced to an insufficient description of dispersion. Consequently, numerous approaches to remedy this deficiency have been explored that have varying degrees of computational and theoretical complexity.[8−32] These methods range from semiempirical C_6/R^6 corrections to more complex vdW corrected functionals, some of which are either computationally infeasible for treating large periodic systems or are not yet implemented for periodic systems. Until recently, these limitations have precluded their use in exploration of energetic molecular solids. However, two recent studies have evaluated the performance of density functional approaches in which van der Waals corrections are included.[33,34] The first, in which two types of corrections (DFT-D and vdW-DF) to DFT are used to calculate energetic and vibrational properties of RDX, shows that both approaches work equally well but the vdW-DF approach requires significantly more computational resources.[33] One of the more important results of this study is its finding that improper treatment of dispersion affects the vibrational properties. This could have profound implications in modeling fundamental processes associated with shock initiation to detonation of an energetic material. Specifically, this would have serious ramifications in theoretical explorations of the phonon up-pumping model of initiation, in which phonons are first excited by passage of a shock wave, followed by a transfer of the energy into molecular vibrations that are coupled with the phonon bath and subsequent "up-pumping" of the higher frequency vibrations.[35] Thus, in such a case it is crucial that both the lattice and molecular vibrational properties be properly described. The second study, in which the same van der Waals correction to DFT (DFT-D) was used to predict crystallographic properties of 10 energetic molecular crystals, produced a similarly good result in predicting the crystallographic lattice parameters at ambient

Received: August 16, 2010
Revised: December 2, 2010
Published: January 20, 2011

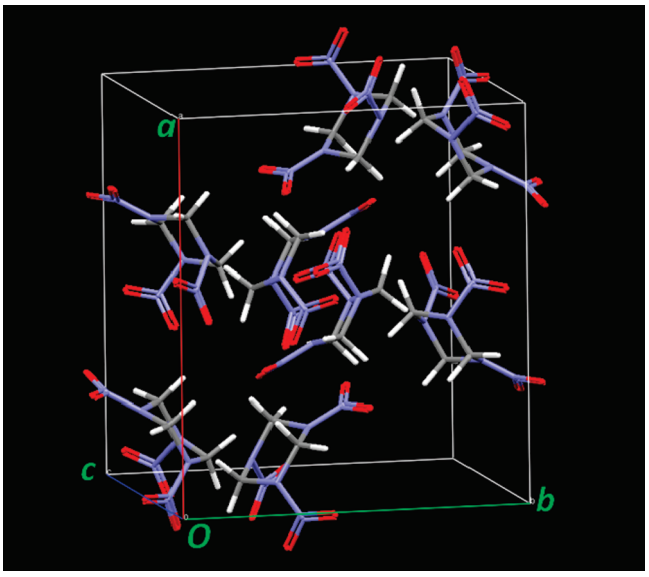

Figure 1. Experimental unit cell for RDX, containing 8 molecules/(unit cell) with *Pbca* symmetry and lattice parameters: a = 13.182 Å, b = 11.574 Å, c = 10.709 Å, and $\alpha = \beta = \gamma = 90°$.[55]

pressure.[34] Application of the method to six of these crystals under hydrostatic compression conditions also showed improvement over the conventional DFT results, and resulting lattice parameters were in good agreement with experimental values.

An alternative approach to the aforementioned methods for correction of the vdW forces is one in which the pseudopotential, as opposed to the explicit functional form, is adjusted to correct for dispersion. These methods consist of the addition of functions to either the effective core potentials[36−42] (in gas-phase codes) or the pseudopotentials[43] (in periodic solid-state codes) in order to correct for van der Waals forces. One such method, dispersion corrected atom centered pseudopotentials (DCACP)[43] is currently implemented in the periodic CP2K program package.[44] The DCACP method uses an additive effective pseudopotential consisting of optimized nonlocal high-order angular momentum terms to correct for the long-range interaction errors seen in standard DFT functionals. These effective pseudopotentials have been implemented in the pseudopotential library provided by Goedecker et al.[45] Each atomic pseudopotential contains a local term and an angular momentum dependent nonlocal term that has been chosen to act at a length scale that differs from that of the local term. The tunable parameters of the nonlocal term (written in Gaussian radial projectors on spherical harmonics) have parametrized against highly accurate wave function based methods for specific calibration systems. While only expanding the nonlocal term in a single channel (angular momentum $l = 3$), this methodology has shown considerable success in treating dispersion in organic and biomolecular systems[46,47] and has demonstrated diverse applicability while maintaining the reduced computational costs associated with DFT calculations when compared to the more theoretically rigorous wave function based calculations. While there have been some deviations from the true asymptotic behavior at longer ranges, the single-channel DCACP methodology was designed specifically to treat midrange van der Waals interactions and should be well suited for the study of condensed-phase molecular systems.[48−50] For these reasons (the ability to treat large periodic systems and reasonable accuracy for other vdW systems) we have performed a study to assess the suitability of DCACPs in prediction of crystal-

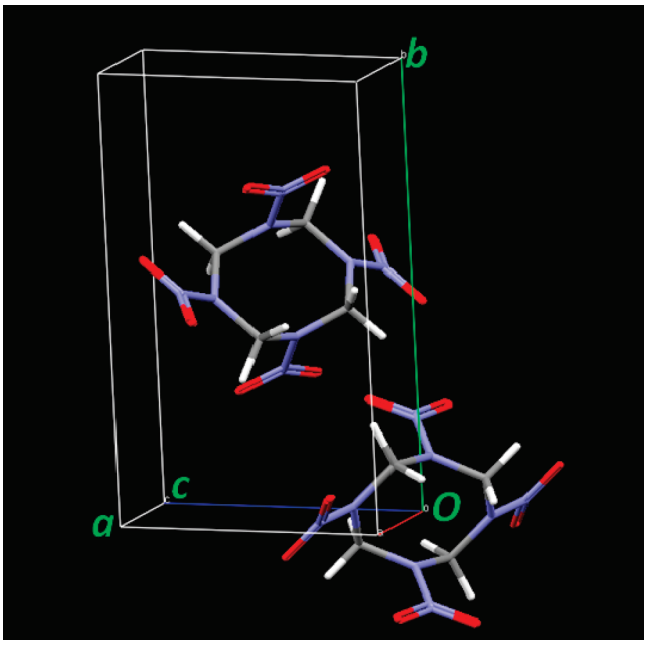

Figure 2. Experimental unit cell for β-HMX, containing 2 molecules/(unit cell) with $P2_1/n$ symmetry and lattice parameters: a = 6.54 Å, b = 11.05 Å, c = 8.7 Å, $\alpha = \gamma = 90°$, and $\beta = 124.3°$.[56]

lographic and molecular structural parameters of four important energetic molecular crystals: cyclotrimethylenetrinitramine (RDX), 1,3,5,7-tetranitro-1,3,5,7-tetraazacyclooctane (HMX), 2,4,6-trinitro-1,3,5-benzenetriamine (TATB), and pentaerythritol tetranitrate (PETN) at ambient pressure (Figures 1−4).

2. COMPUTATIONAL DETAILS

Crystal structures were obtained through geometry optimizations using the generalized gradient approximation (GGA) density functional Perdew−Burke−Ernzerhof (PBE)[51] and two types of pseudopotentials within the CP2K solid-state DFT package, version 2.0.0.[44] The first is the standard Goedecker−Teter−Hutter (GTH) pseudopotential;[52] all calculations using this pseudopotential will be denoted as "DFT" hereafter. The second used in this study is the dispersion corrected atom centered pseudopotential;[43] all calculations using this pseudopotential will be denoted as "DCACP" hereafter. All the calculations were performed at the Γ point of the Brillouin zone and used Gaussian triple-ζ valence basis sets (TZVP) as well as an auxiliary plane wave basis set. In each calculation, a full-dimensional variable cell optimization at ambient pressure was performed using the conjugate gradient (CG) method for optimizing the cell degrees of freedom and Broyden−Fletcher−Goldfarb−Shanno (BFGS) optimizer for the ionic degrees of freedom. The initial crystal and molecular parameters for RDX (Figure 1), β-HMX (Figure 2), TATB (Figure 3), and PETN (Figure 4) used in the geometry optimization correspond to experimentally measured values.[53−56]

To ensure that k-space was sufficiently described for the DCACP method, DCACP calculations were performed at 2000 Ry for the crystals with small edge lengths (i.e., HMX, PETN, and TATB) using supercells composed of 2 × 2 × 2 unit cells. The results for HMX and PETN differed from calculations using the single unit cells by a maximum of ~0.02 Å; therefore all subsequent calculations for these systems used a single unit cell. The results for TATB using the unit cell and supercell were dramatically different: crystal

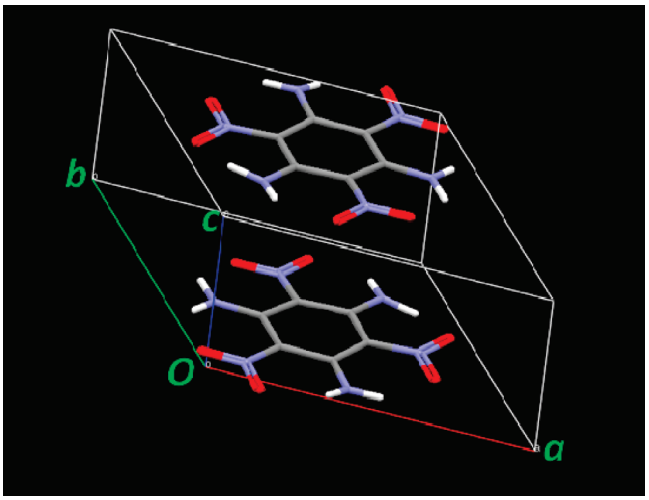

Figure 3. Experimental unit cell for TATB, containing 2 molecules/(unit cell) with $P\bar{1}$ symmetry and lattice parameters: a = 9.01 Å, b = 9.028 Å, c = 6.812 Å, α = 108.58°, β = 91.82°, and γ = 119.97°.[53]

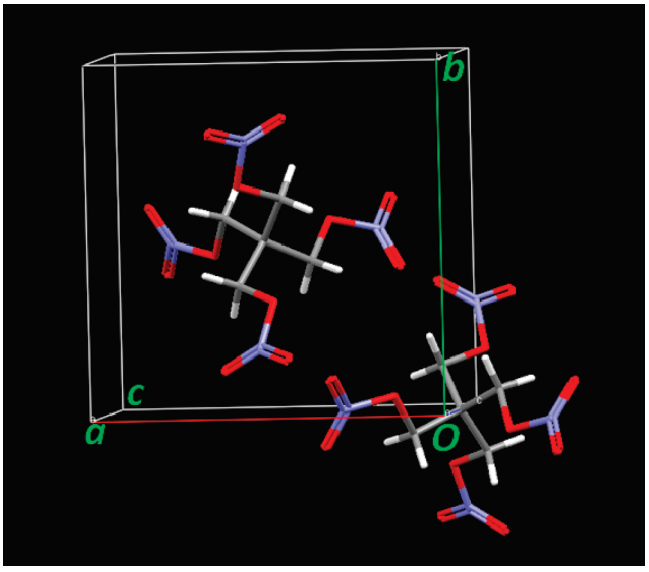

Figure 4. Experimental unit cell for PETN, containing 2 molecules/(unit cell) with $P4_21c$ symmetry and lattice parameters: $a = b$ = 9.303 Å, c = 6.64 Å, and $\alpha = \beta = \gamma$ = 90°.[54]

parameters differed by ~3.5%, and one of the cell angles differed by 4°. Therefore, all TATB calculations reported herein used a 2 × 2 × 2 supercell. For each system, variable cell optimizations at plane wave cutoffs of 700, 1000, 1200, 1400, 1600, 1800, and 2000 Ry were performed to determine convergence with respect to basis set size. The convergence criteria were set to 0.02 au for maximum change in the geometry, 0.001 hartree·bohr^{-1} for maximum change in energy gradient component, and 100 bar for pressure change between successive iterations. Tighter convergence criteria (factor of 10 for the maximum change in energy gradients and geometries) were required to obtain convergence for PETN at 1400 Ry.

3. RESULTS AND DISCUSSION

3.1. Lattice Parameter and Energy Analysis. Figures 5−8 show DCACP and DFT lattice vectors and volumes for RDX, HMX, PETN, and TATB as functions of basis set size. Detailed crystallographic data for all calculations are given in Table 1S (see Supporting Information). The DCACP volume for HMX converges to a final value as basis set size is increased, while RDX, TATB, and PETN values show an approximate convergence with basis set size. Further exploration of convergence with ever larger basis sets, while desirable, are beyond the scope of this project, as DCACP values for the volumes at the largest basis set are all within ~2% of the experimental value. All DCACP calculations underestimate the volume at small basis set sizes and overestimate the volumes as the basis set size increases. In contrast, the HMX and PETN DFT volumes did not converge with increasing basis set size while RDX and TATB showed a rough convergence. Moreover, the DFT volumes are always overestimated with respect to the experimental values (except for HMX at 700 Ry). The errors in the DFT volumes at 2000 Ry were as low as 5% in the case of HMX and as high as 10% for TATB. One notable feature of the DFT calculations is that the calculated volumes at 700 Ry are very close to the experimental values, with the error being less than 1% for all systems except TATB, where the error is ~4%.

DCACP predictions of lattice vector lengths using the largest basis set are within 1% of experiment except for TATB, which has a maximum error of 1.3%. The errors in the cell angles at the largest basis set are within a hundredth of a degree except in the case of TATB where the deviation is as high as 2.2°. DFT lattice vector lengths using the largest basis set are within 2.5% of the experimental values, with TATB exhibiting the largest deviation in cell angles of −6.0°. The increased error in the cell lengths coupled with the error in the cell angle results in the large deviation from the experimental volume for TATB. All cell angles for the other systems are in reasonably good agreement with experiment, with the largest absolute deviation being 0.9° for HMX (please refer to the Supporting Information for specific data points).

The aforementioned DFT-D study of Sorescu and Rice[34] provides an opportunity to compare two disparate methods that address the lack of dispersion in conventional DFT. The DFT-D results discussed herein were calculated using the PBE functional[51] and Vanderbilt ultrasoft pseudopotentials[57] as implemented in the plane wave electronic structure code PWscf[58] within Quantum-ESPRESSO.[59] DFT-D values calculated using an 80 Ry kinetic energy cutoff will be compared with DCACP values using a 2000 Ry kinetic energy cutoff. While the large difference in the size of the kinetic energy cutoff might suggest such a comparison is not meaningful, we remind the reader that the DFT-D method used the Vanderbilt ultrasoft pseudopotentials, allowing for a significant reduction in the number of plane waves required for convergence, whereas a "hard" pseudopotential, such as the Goedecker−Teter−Hutter pseudopotential employed for the DCACP method, requires a larger number of plane waves to achieve convergence. Visual comparison of the volumes and lattice vector lengths are provided in Figures 5−8 with the triangles denoting the DFT-D results. Both studies show an improvement over conventional DFT, with all lattice parameters being within 2% of the experimental information. For all systems, the DFT-D volumes are smaller than the DCACP volumes and, with the exception of PETN, are all smaller than the experimental volumes. However, a closer inspection of the lattice parameters shows that a fortuitous cancellation of errors is the cause of the low errors in the predicted DFT-D volumes. For RDX, the DFT-D lattice vector lengths are all smaller than

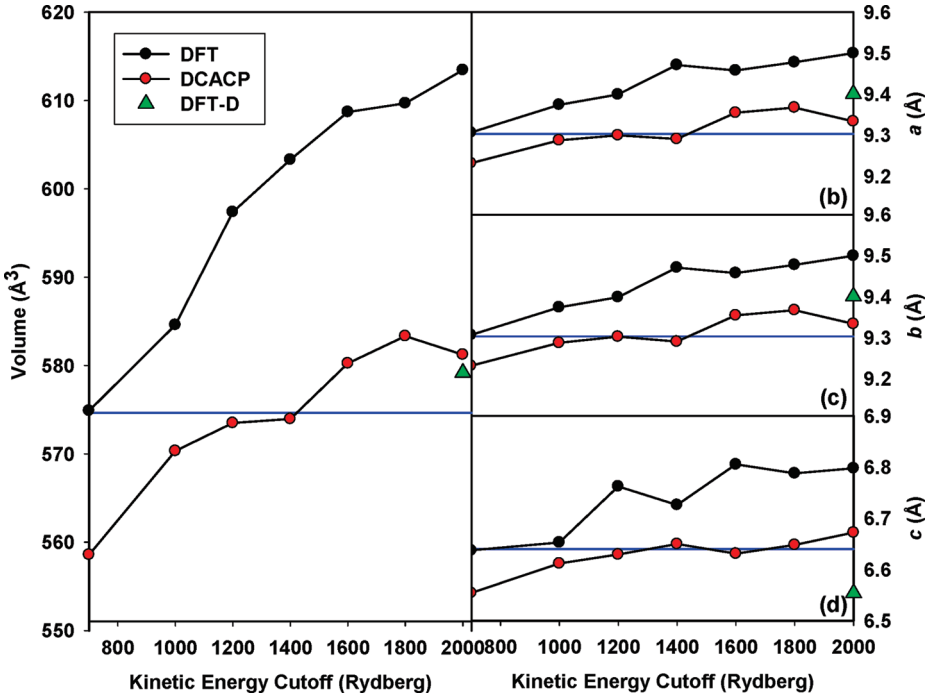

Figure 5. Crystallographic parameters as a function of kinetic energy cutoffs for RDX: (a) volume; (b) cell edge length *a*; (c) cell edge length *b*; (d) cell edge length *c*. Experimental values are denoted by the horizontal lines.

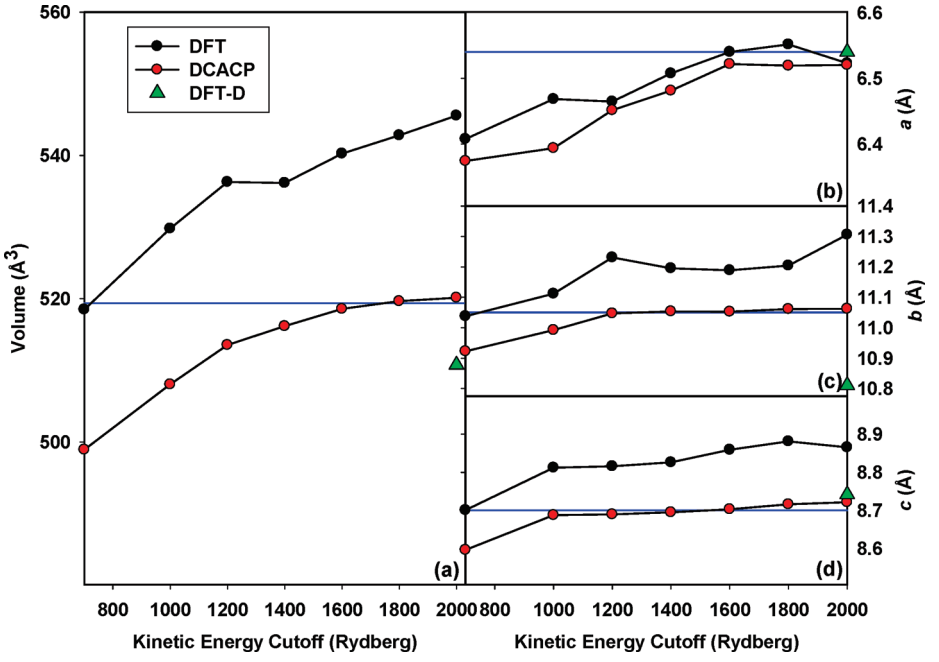

Figure 6. Crystallographic parameters as a function of kinetic energy cutoffs for HMX: (a) volume; (b) cell edge length *a*; (c) cell edge length *b*; (d) cell edge length *c*. Experimental values are denoted by the horizontal lines.

DCACP values. In particular the *b* lattice vector calculated using DFT-D is smaller than the experimental value by 1.6%, whereas the DCACP value is larger by 0.1%. The DFT-D results for β-HMX also has a larger deviation from the experimental *b* lattice vector by ~2% and is the main source of the underprediction of the experimental volume. Both methods predict the non-90° angle of this monoclinic crystal to within 0.15°. For PETN, DFT-D and DCACP volumes overestimate the experimental volume by approximately the same amount. However, the three DCACP lattice vectors overpredict the experimental values by 0.2−0.6%, whereas the DFT-D values overpredict lattice vectors *a* and *b* by 1.35% and underpredict the *c* lattice vectors by −0.89%. Conversely, for TATB the DCACP and DFT-D lattice vectors are in almost exact agreement with one another, but the volumes differ significantly. As previously mentioned, the DCACP volume is overpredicted by 2.3%, and the DFT-D value underpredicts the

dx.doi.org/10.1021/jp107760k |*J. Phys. Chem. B* 2011, 115, 803–810

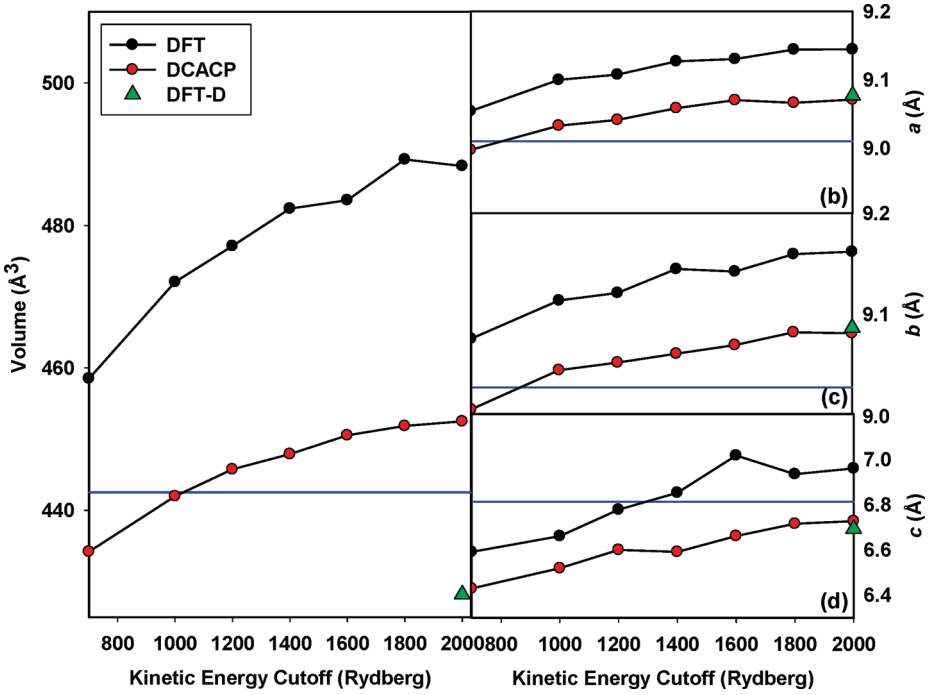

Figure 7. Crystallographic parameters as a function of kinetic energy cutoffs for TATB: (a) volume; (b) cell edge length *a*; (c) cell edge length *b*; (d) cell edge length *c*. Experimental values are denoted by the horizontal lines.

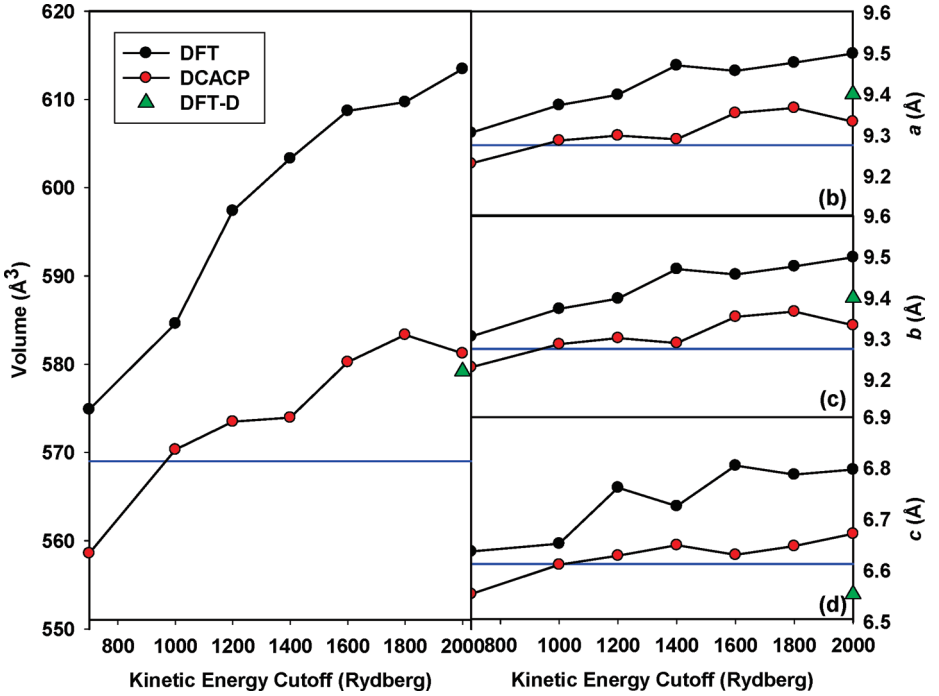

Figure 8. Crystallographic parameters as a function of kinetic energy cutoffs for PETN: (a) volume; (b) cell edge length *a*; (c) cell edge length *b*; (d) cell edge length *c*. Experimental values are denoted by the horizontal lines.

volume by 3.2%. This error is due to the differences in predictions of one of the three non-90° angles in this triclinic unit cell. The DCACP value is 106.35°, which is 2.23° smaller than the experimental value, while the DFT-D value is 111.82°, which is 2.98° larger than experiment (please refer to the Supporting Information for specific data points). These results correspond to a 0 K result and do not include thermal effects; therefore, we cannot conclude with absolute certainty that one method is more suitable than the other. Rather, both approaches appear to be reasonable methods to predict crystallographic structures of energetic molecular crystals, with the DCACP method usually yielding more accurate lattice vectors over those predicted from DFT-D.

Cohesive energies for each molecule at the largest energy cutoff can be found in Table 1 for both the DCACP and DFT

dx.doi.org/10.1021/jp107760k |*J. Phys. Chem. B* 2011, 115, 803–810

Table 1. Cohesive Energy per Molecule (kcal/mol) for Both the DFT and DCACP Methods, as Well the Difference, at 2000 Ry for RDX, β-HMX, TATB, and PETN

molecule	DFT	DCACP	DCACP-DFT
RDX	−15.21	−20.72	−5.52
β-HMX	−21.04	−27.78	−6.74
TATB	−15.80	−24.93	−9.13
PETN	−13.60	−20.03	−6.43

methods. For each system, we compute the cohesive energy by $\Delta E = E_{bulk}/N_{molecule} - E_{molecule}$, where $N_{molecule}$ is the number of molecules used in the calculation of the crystal material and E_{bulk} and $E_{molecule}$ are the crystal and individual molecule energies, respectively. The energy of the individual molecule was computed using the 2000 Ry plane wave cutoff. As seen in Table 1, the DCACP calculations have a larger binding energy per molecule than do the DFT calculations. For the TATB molecule, which shows the greatest improvement in predicted volume when using the DCACP method, we also observe the largest difference in the cohesive energy between the two methods.

3.2. Structural Analysis at the Molecular Level. Molecular parameters (i.e., the centers-of-mass translational and orientational degrees of freedom) of the systems were also calculated to evaluate the relative predictive capabilities of DFT and DCACP methods. In our discussions the translational degrees of freedom will be expressed as fractional coordinates (*sx*, *sy*, *sz*) of the molecular centers of mass. Euler angles (θ, φ, ψ) describing rigid-body rotations of molecules about the inertial axes will be used to describe the orientational degrees of freedom. While performing the variable cell optimization, symmetry constraints were not imposed. Consequently, the results and the discussions will be presented for each of the symmetry-equivalent molecules or, in the case of PETN, asymmetric units in the unit cell.

We used the method proposed by Kearsley[60] to perform the analysis on molecular degrees of freedom. This procedure involves superimposing the calculated and experimental unit cells and then determining the deviations in the molecular degrees of freedom; details are given in our earlier study.[6] The root-mean-square and maximum deviations of the atomic positions and the translational and rotational degrees of freedom for the molecules are listed in Tables 2S−9S (see the Supporting Information).

The DFT and DCACP molecular parameters for the RDX system and their deviations from the experimental parameters are listed in Tables 2S and 3S (see the Supporting Information), respectively. RDX belongs to the *Pbca* space group; thus, its unit cell has 8 symmetry equivalent molecules with each composed of 21 atoms. Calculated molecular parameters at both levels of theory show little dependence on kinetic energy cutoff, and the deviations from the experiments are low. Fractional coordinates and Euler angles are in good agreement with experiment for all calculations, with the DCACP predictions being only slightly better than the DFT calculations (see Table 2 for maximum atomic displacements and RMS errors for both DFT and DCACP at 2000 Ry). Similarly to RDX, for calculations on the monoclinic system β-HMX (belonging to the $P2_1/n$ space group with each unit cell containing two molecules each with 28 atoms), both levels of theory show little dependence on kinetic energy cutoff, and the DCACP calculations are only slightly better than the DFT (Tables 4S and 5S (see the Supporting Information)). The predicted translational degrees of freedom are in very good agreement with

Table 2. Maximum Atomic Displacements and Root Mean Square Errors (RMSE) for Both the DFT and DCACP Methods at 2000 Ry for RDX, β-HMX, TATB, and PETN

	DFT		DCACP	
molecule	max displ (Å)	max RMSE (Å)	max displ (Å)	max RMSE (Å)
RDX	0.217	0.165	0.110	0.069
β-HMX	0.421	0.187	0.382	0.145
TATB	0.676	0.496	0.435	0.243
PETN[a]	0.216	0.165	0.149	0.085

[a] Evaluation of PETN was performed on the asymmetric subunit rather than the overall molecule.

the experiment, differing only in the hundredths of fractional units for both levels of theory. These small differences are apparent in Table 2, with the methods within close agreement with each other and experiment. The Euler angles are not as well predicted at either level of theory and deviate from experiment by 2−4°.

For TATB (a near-planar molecule belonging to the triclinic $P\bar{1}$ space group, containing two molecules of 24 atoms each in the unit cell), however, initial efforts at comparing predicted and experimental structures result in a potentially misleading analysis. While the predicted translational degrees of freedom for both levels of theory differ in the hundredths from the experimental values and have a minimal dependence on the kinetic energy cutoffs, direct comparison of the molecular orientational parameters with experiment is deceptive and at first glance appears to show large deviations. However, as we showed in a previous study,[6] one of the inertial axes for TATB is perpendicular to the plane of the molecule (Euler angle θ in Tables 6S and 7S (see the Supporting Information)), and the remaining two inertial axes lie within the plane of the molecules (Euler angles ϕ and ψ). Our previous study demonstrated that these differences in these two inertial axes (due to the symmetry of the molecule) do not affect the overall molecular orientation within the unit cell, as seen in the superposition of the predicted supercell onto the experimental counterpart in Figure 9.[6] Table 2 illustrates the error for both methodologies, with the predicted DCACP values showing improvement over the DFT results at 2000 Ry.

Finally, for PETN, a prolate symmetric top molecule belonging to the $P4_21c$ space group, further difficulties in analysis arise. The unit cell has two molecules, each with 29 atoms, with the asymmetric unit consisting of 8 atoms. Extraction of Euler angles from this system produces $\theta = 90°$; the two remaining Euler angles are interrelated, and no unique solution exists. As in our previous study,[6] to compare molecular orientational parameters among the levels of theory, kinetic energy cutoffs, and experimental values, we have analyzed the molecular parameters for each of the symmetry equivalent asymmetric units of the PETN unit cell, rather than the overall molecule. The experimental, DFT, and DCACP translational and orientational degrees of freedom for the symmetric equivalents of the asymmetric unit are listed in Tables 8S and 9S (see the Supporting Information) and show a very weak dependence on kinetic energy cutoffs. Both translational and orientational degrees of freedom are in reasonably good agreement with experiment for both levels of theory and for all kinetic energy cutoffs as seen in Table 2 and the Supporting Information.

For the structural molecular parameters, the centers-of-mass translational and orientational degrees of freedom, it is apparent

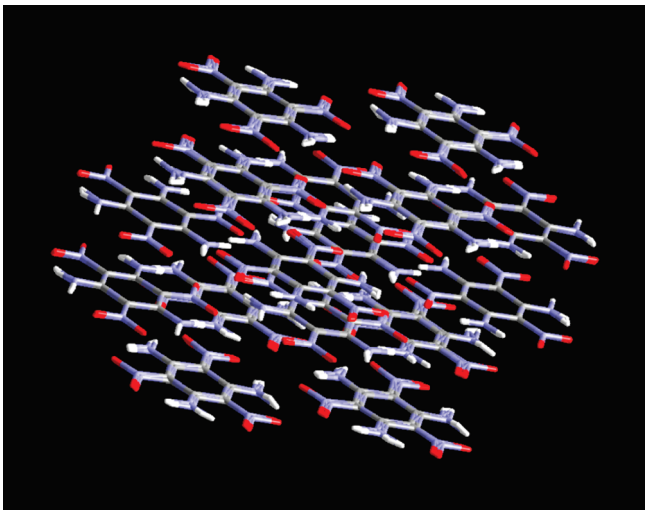

Figure 9. Superimposed DCACP and experimental unit cells for TATB.

that the DCACP method yields smaller maximum displacements and root-mean-square errors than the DFT method. While in some cases the differences are minute (β-HMX), for others, specifically RDX and PETN, DCACP lowers the RMS error by approximately a factor of 2.

4. CONCLUSIONS

The performance of dispersion corrected atom centered pseudopotentials was evaluated through a comparative study against conventional DFT calculations of the structural features of four molecular crystals at ambient pressure. Both crystallographic and molecular structural parameters were calculated, with the largest differences between DCACP and DFT calculations shown to be in the lattice vector lengths; molecular structural parameters displayed little dependency on the pseudopotential. For all four systems, the DCACP predictions of lattice vector lengths and volumes are more accurate than those using conventional DFT calculations. While DCACP calculations showed convergence of volume and lattice vector lengths with increasing kinetic energy cutoffs, the DFT values did not always converge. DCACP crystallographic parameters were in overall good agreement with experimental values for all systems; lattice vector lengths are within 1.3% of experiment, corresponding to ~2% error in density. Comparison with similar calculations using the DFT-D approach[18,34] indicate that the DCACP methodology is a more accurate method to correct for lack of van der Waals interactions in conventional DFT. These results also suggest that although DCACPs were not explicitly constructed to capture the theoretically correct asymptotic r^{-6} long-range attractive behavior (unlike the DFT-D methodology), their "medium range" description is sufficient to model the interactions of some molecular crystal systems that were inadequately described using conventional DFT. This hypothesis could be further tested through the use of the recently developed multichannel DCACP methodology, which has shown the correct asymptotic r^{-6} behavior for the hydrogen molecule dimer without explicitly imposing this functional form in the pseudopotential.[61] This lack of explicit two-body behavior may actually be the reason the DCACP methodology outperforms the DFT-D method, as recent studies have shown higher order many body effects can be of critical importance to the proper description of van der Waals systems.[62,63] As DCACPs are parametrized to reference systems containing many-body effects and have not been explicitly constructed to include only the two-body contributions, as DFT-D has been, it is possible that that these higher order effects have been approximately captured, resulting in better predicted lattice vectors. A study determining exactly how well the DCACP methodology (both one channel and multichannel) describes many-body effects would be ideal in resolving this question.

■ ASSOCIATED CONTENT

Supporting Information. Tables listing crystallographic parameters of RDX, HMX, TATB, and PETN and DFT and DCACP crystallographic and molecular structural parameters for RDX, β-HMX, TATB, and PETN. This material is available free of charge via the Internet at http://pubs.acs.org.

■ AUTHOR INFORMATION

Corresponding Author
*E-mail: edward.fc.byrd@us.army.mil.

■ ACKNOWLEDGMENT

Calculations were performed using the DOD Supercomputing Resource Centers (DSRCs) located at the U.S. Army Research Laboratory, the U.S. Army Engineer Research and Development Center, and the Air Force Research Laboratory. R.B. was supported by an appointment to the Internship/Research Participation Program for the U.S. Army Research Laboratory administered by the Oak Ridge Institute for Science and Education through an agreement between the U.S. Department of Energy and the USARL.

■ REFERENCES

(1) Rice, B. M.; Byrd, E. F. C.; Mattson, W. D. *Struct. Bonding (Berlin, Germany)* **2007,** *125,* 153–194.
(2) Hafner, J.; Wolverton, C.; Ceder, G. *Mat. Res. Soc. Bull.* **2006,** *31,* 659.
(3) Oxtoby, D. W. *Annu. Rev. Mater. Sci.* **2002,** *32,* 39.
(4) Wu, J.; Li, Z. *Annu. Rev. Phys. Chem.* **2007,** *58,* 85.
(5) Martin, R. M. *Electronic Structure: Basic Theory and Practical Methods*; Cambridge University Press: Cambridge, U.K., 2004.
(6) Byrd, E. F. C.; Scuseria, G. E.; Chabalowski, C. F. *J. Phys. Chem. B* **2004,** *108,* 13100.
(7) Byrd, E. F. C.; Rice, B. M. *J. Phys. Chem. C* **2007,** *111,* 2787.
(8) Conway, A.; Murrell, J. N. *Mol. Phys.* **1974,** *27,* 873.
(9) Wagner, A. F.; Das, G.; Wahl, A. C. *J. Chem. Phys.* **1974,** *60,* 1885.
(10) Hepburn, J.; Scoles, G.; Penco, R. *Chem. Phys. Lett.* **1975,** *36,* 451.
(11) Ahlrichs, R.; Penco, R.; Scoles, G. *Chem. Phys.* **1977,** *19,* 119.
(12) Craig, D. P.; Thirunamachandran, T. *Molecular Quantum Electrodynamics*; Dover: Mineola, NY, 1998.
(13) Rydberg, H.; Lundqvist, B. I.; Langreth, D. C.; Dion, M. *Phys. Rev. B* **2000,** *62,* 6997.
(14) Rydberg, H.; Dion, M.; Jacobsen, N.; Schröder, E.; Hyldgaard, P.; Simak, S. I.; Langreth, D. C.; Lundqvist, B. I. *Phys. Rev. Lett.* **2003,** *91,* 126402.
(15) Wesolowski, T. A.; Tran, F. *J. Chem. Phys.* **2003,** *118,* 2072.
(16) Meijer, E. J.; Sprik, M. *J. Chem. Phys.* **1996,** *105,* 8684.
(17) Elstner, M.; Hobza, P. *J. Chem. Phys.* **2001,** *114,* 5149.
(18) Grimme, S. *J. Comput. Chem.* **2006,** *27,* 1787.
(19) Wu, X.; Vargas, M. C.; Nayak, S.; Lotrich, V.; Scoles, G. *J. Chem. Phys.* **2001,** *115,* 8748.

(20) Ortmann, F.; Bechstedt, F.; Schmidt, W. G. *Phys. Rev. B* **2006,** *73*, 205101.
(21) Douketis, C.; Scoles, G.; Marchetti, S.; Zen, M.; Thakkar, A. J. *J. Chem. Phys.* **1982,** *76*, 3057.
(22) Silvestrelli, P. L. *Phys. Rev. Lett.* **2008,** *100*, 053002.
(23) Kohn, W.; Meir, Y.; Makarov, D. E. *Phys. Rev. Lett.* **1998,** *80*, 4153.
(24) Dion, M.; Rydberg, H.; Schröder, E.; Langreth, D. C.; Lundqvist, B. I. *Phys. Rev. Lett.* **2004,** *92*, 246401.
(25) Langreth, D. C.; Dion, M.; Rydberg, H.; Schröder, E.; Hyldgaard, P.; Lundqvist, B. I. *Int. J. Quantum Chem.* **2005,** *101*, 599.
(26) Schwabe, T.; Grimme, S. *Phys. Chem. Chem. Phys.* **2007,** *9*, 3397.
(27) Hooper, J.; Cooper, V. R.; Thonhauser, T.; Romero, N. A.; Zerilli, F.; Langreth, D. C. *ChemPhysChem* **2008,** *9* (6), 891.
(28) Hult, E.; Rydberg, H.; Lundqvist, B. I.; Langreth, D. C. *Phys. Rev. B* **1999,** *59*, 4708.
(29) Dobson, J. F.; Dinte, B. P. *Phys. Rev. Lett.* **1996,** *76*, 1780.
(30) Thonhauser, T.; Cooper, V. R.; Li, S.; Puzder, A.; Hyldgaard, P.; Langreth, D. C. *Phys. Rev. B* **2007,** *76*, 125112.
(31) Vydrov, O. A.; Wu, Q.; Voorhis, T. V. *J. Chem. Phys.* **2008,** *129*, 14106.
(32) Artacho, E.; Anglada, E.; Dieguez, O.; Gale, J. D.; Garcia, A.; Junquera, J.; Martin, R. M.; Ordejon, P.; Pruneda, J. M.; Sanchez-Portal, D.; Soler, J. M. *J. Phys.: Condens. Matter* **2008,** *20*, 6.
(33) Shimojo, F.; Wu, Z.; Nakano, A.; Kalia, R. K.; Vashishta, P. *J. Chem. Phys.* **2010,** *132*, 094106.
(34) Sorescu, D. C.; Rice, B. M. *J. Phys. Chem. C* **2010,** *114*, 6734.
(35) Dlott, D. D. Multiphonon up-pumping in energetic materials. In *Overviews of Recent Research on Energetic Materials*; Thompson, D., Brill, T., Shaw, R., Eds.; World Scientific: Hackensack, NJ, 2005; p 303.
(36) DiLabio, G. A. *Chem. Phys. Lett.* **2008,** *45*, 348.
(37) Mackie, I. D.; DiLabio, G. A. *J. Chem. Phys.* **2008,** *112*, 10968.
(38) Mackie, I. D.; McClure, S. A.; DiLabio, G. A. *J. Phys. Chem. A* **2009,** *113*, 5476.
(39) DiLabio, G. A.; Johnson, E. R.; Pitters, J. *J. Phys. Chem. C* **2009,** *113*, 9970 (Letter).
(40) Johnson, E. R.; Mackie, I. D.; DiLabio, G. A. *J. Phys. Org. Chem.* **2009,** *22*, 1127.
(41) Mackie, I. D.; DiLabio, G. A. *Phys. Chem. Chem. Phys.* **2010,** *12*, 6092.
(42) McClure, S. A.; Buriak, J. M.; DiLabio, G. A. *J. Phys. Chem. C* **2010,** *114*, 10952.
(43) von Lilienfeld, O. A.; Tavernelli, I.; Rothlisberger, U.; Sebastiani, D. *Phys. Rev. Lett.* **2004,** *93*, 153004.
(44) CP2K Developers Group. *CP2K Code*, http://cpk2.berlios.de, 2000−2006).
(45) Hartwigsen, C.; Goedecker, S.; Hutter, J. *Phys. Rev. B* **1998,** *58*, 3641.
(46) Tapavicza, E.; Lin, I.-C.; von Lilienfeld, O. A.; Tavernelli, I.; Coutinho-Neto, M. D.; Rothlisberger, U. *J. Chem. Theory Comput.* **2007,** *3*, 1673.
(47) Lin, I.-C.; Rothlisberger, U. *Phys. Chem. Chem. Phys.* **2008,** *10*, 2730.
(48) von Lilienfeld, O. A.; Tavernelli, I.; Rothlisberger, U.; Sebastiani, D. *Phys. Rev. B* **2005,** *71*, 195119.
(49) Lin, I.-C.; von Lilienfeld, O. A.; Coutinho-Neto, M. D.; Tavernelli, I.; Rothlisberger, U. *J. Phys. Chem. B* **2007,** *111*, 14346.
(50) Lin, I.-C.; Rothlisberger, U. *Phys. Chem. Chem. Phys.* **2008,** *10*, 2730.
(51) Perdew, J. P.; Burke, K.; Ernzerhof, M. *Phys. Rev. Lett.* **1996,** *77*, 3865.
(52) oedecker, S.; Teter, M.; Hutter, J. *Phys. Rev. B* **1996,** *54*, 1703.
(53) Cady, H. H.; Larson, A. C. *Acta Crystallogr.* **1965,** *18*, 485.
(54) Nieger, M.; Lehmann, J. Private communication, CSD Refcode PERYTN11, 2002.
(55) Choi, C. S.; Prince, E. *Acta Crystallogr., Sect. B* **1972,** *28*, 2857.
(56) Choi, C. S.; Boutin, H. P. *Acta Crystallogr., Sect .B* **1970,** *26*, 1235.
(57) Vanderbilt, D. *Phys. Rev. B* **1990,** *41*, 7892.
(58) Barone, V.; Casarin, M.; Forrer, D.; Pavone, M.; Sambi, M.; Vittadini, A. *J. Comput. Chem.* **2009,** *30*, 934.
(59) Giannozzi, P.; Baroni, S.; Bonini, N.; Calandra, M.; Car, R.; Cavazzoni, C.; Ceresoli, D.; Chiarotti, G. L.; Cococcioni, M.; Dabo, I.; Dal Corso, A.; de Gironcoli, S.; Fabris, S.; Fratesi, G.; Gebauer, R.; Gerstmann, U.; Gougoussis, C.; Kokalj, A.; Lazzeri, M.; Martin-Samos, L.; Marzari, N.; Mauri, F.; Mazzarello, R.; Paolini, S.; Pasquarello, A.; Paulatto, L.; Sbraccia, C.; Scandolo, S.; Sclauzero, G.; Seitsonen, A. P.; Smogunov, A.; Umari, P.; Wentzcovitch, R. M. *J. Phys.: Condens. Matter* **2009,** *21*, 395502.
(60) Kearsley, S. K. *Acta Crystallogr., Sect. A* **1989,** *45*, 208.
(61) Tavernelli, I.; Lin, I.-C.; Rothlisberger, U. *Phys. Rev. B* **2009,** *79*, 045106.
(62) Tkatchenko, A.; von Lilienfeld, O. A. *Phys. Rev. B* **2008,** *78*, 045116.
(63) von Lilienfeld, O. A.; Tkatchenko, A. *J. Chem. Phys.* **2010,** *132*, 234109.